Journal of Applied Physics ARTICLE pubs.aip.org/aip/jap

Study of pristine and degraded blue quantum dot light-emitting diodes by transient electroluminescence measurements

Cite as: J. Appl. Phys. **135**, 045701 (2024); doi: 10.1063/5.0180211
Submitted: 8 October 2023 · Accepted: 16 December 2023 ·
Published Online: 22 January 2024

Wenxin Lin,[1] Jiangxia Huang,[1] Shuxin Li,[1] Paul W. M. Blom,[2] Haonan Feng,[1] Jiahao Li,[1] Xiongfeng Lin,[3] Yulin Guo,[3] Wenlin Liang,[3] Longjia Wu,[3] Quan Niu,[1,a)] and Yuguang Ma[1]

AFFILIATIONS

[1]State Key Laboratory of Luminescent Materials and Devices, South China University of Technology, 510006 Guangzhou, China
[2]Max Planck Institute for Polymer Research, 55128 Mainz, Germany
[3]TCL Corporate Research, 518067 Shenzhen, China

[a)]**Author to whom correspondence should be addressed:** qqniu@scut.edu.cn

ABSTRACT

Limited stability of blue quantum dot light-emitting diodes (QLEDs) under current stress impedes commercialization. Multi-layer structures of the state-of-the-art blue QLEDs pose significant difficulty in the fundamental understanding of degradation mechanisms. Here, by applying transient electroluminescence measurements, we disentangle charge transport in both pristine and degraded blue QLEDs. By varying thicknesses of the charge transport layers and the emissive layer, respectively, we show that the charge transport in pristine QLEDs is primarily dominated by holes. Furthermore, the degradation of QLEDs under electrical stress is governed by the decrease of hole transport in the emissive quantum dot layer due to the formation of hole traps.

I. INTRODUCTION

Quantum dot light-emitting diodes (QLEDs) are attractive for next-generation display and lighting technologies owing to their potential for low-cost fabrication, high color purity, and wide color gamut.[1,2] Considerable efforts have been made to improve their lifetime and efficiency, and market-desirable high-performance green and red QLEDs have been realized.[3–7] So far, for red and green devices, the T_{95} operational lifetime defined as the time for luminescence to degrade to 95% of the initial luminescence of 1000 cd/m^2 has exceeded 7000 h.[3,7] Nevertheless, blue QLEDs with a lifetime comparable to those of red and green QLEDs have not been realized yet. For the state-of-the-art blue QLEDs, the T_{95} operational lifetime at an initial luminescence of 1000 cd/m^2 is 57 h, which is far away from the demands for commercialization.[3] Extensive research has been conducted to investigate the degradation mechanism of QLEDs in order to achieve stable blue QLEDs.

For instance, to understand which type of charge carriers will play a critical role in the degradation process of QLEDs, the effects of electrical stress on single-carrier devices based on CdSe/CdS quantum dots (QDs) capped with Cd(RCOO)$_2$ were investigated.[4] It was observed that the hole-only device maintained unchanged photoluminescence (PL) efficiency of QDs under electrical stress but the electron-only device and QLEDs showed a significant decline in PL efficiency, which led to the conclusion that the decrease in the photoluminescence of QDs during device aging is primarily caused by the presence of electrons. Given the inner inorganic lattice of a QD is electrochemically stable, the electrochemical degradation of QDs in the devices should be associated with their inorganic–ligand interface. It was discussed that this leads to the generation of redox products (Cd^0), which subsequently quench the luminescence of QDs.[4] The influence of interaction between QDs and ligands on the stability of QLEDs was further studied by investigating the lifetime of QLEDs based on QDs capped with different ligands.[2] It was found that a stronger binding energy and more binding bonds promise better stability during device operation and longer lifetime. Another method to investigate the degradation process of QLEDs is using impedance spectroscopy.[2,8,9] Previously, an increase in peak capacitance around built-in voltage

was observed in degraded QLEDs, suggesting that more traps were formed during the operation which further deteriorated device performance.[2]

Apart from the degradation of the emissive layer (EML), the degradation of the charge transport layers under an electric bias has also been reported.[1,3,8,10] For example, a recent study has monitored the electroluminescence (EL) and photoluminescence (PL) characteristics of QLEDs during device aging.[10] It was observed that the photoluminescence of the hole transport layer decreased by aging, leading to the conclusion that the luminance decrease of QLEDs is attributed to the degradation of the hole transport layer (HTL). Furthermore, by using electrochemical *in situ* fluorescence spectroscopy, it was reported that the degradation of the hole transport layer was a result of electrochemical reduction of the hole transport layer, which was caused by electron leakage from the emissive quantum dot layer to the hole transport layer.[10] However, the other study reported that inefficient hole injection could cause charge accumulation in the hole transport layer, resulting in electrochemical oxidation of the hole transport layer. This was supported by the identification of oxidized molecules (HTL^+) using electro-absorption spectra after a lifetime test.[8] A significant increase in driving voltage is often observed during the degradation of QLEDs. To unravel the mechanism behind it, Chen *et al.* analyzed the charge-modulated electro-absorption spectra for the organic hole transport layer, the emissive layer based on CdZnS QDs, and the electron transport layer (ETL), to spot possible space-charge accumulation, which could lead to a voltage rise during aging.[8] It was found that the space-charge accumulation only occurred in samples containing both blue QDs and zinc oxide (ZnO) ETL. Considering the substantial conduction band maximum (CBM) offset between ZnO and QDs due to the shallow CBM of the ZnS shell, it was concluded that the large barrier for electron injection and the electron transfer from QDs to the ZnO electron transport layer resulted in significant charge accumulation during aging. This led to an increased voltage drop across the electron transport layer and contributed to device degradation.[8]

For the state-of-the-art QLEDs, their typical structure consists of the emissive quantum dot layer sandwiched between electron transport layers (ETL), i.e., zinc magnesium oxide (ZnMgO) nanoparticles and hole transport layers (HTL) which are organic semiconductors, i.e., poly((9,9-dioctylfluorenyl-2,7-diyl)-co-{4,4'-[N-(4-sec-butylphenyl) diphenylamine]}) (TFB).[11,12] To understand the degradation mechanism of such multi-layer devices, it is necessary to understand the charge transport and disentangle different mechanisms before and after QLEDs aging. Transient electroluminescence (TEL) measurement is a powerful tool to investigate the charge transport process in pristine and degraded QLEDs.[13–15] Previously, it has been successfully employed in multilayer blue phosphorescent organic light-emitting diodes to disentangle the charge transport and investigate their degradation mechanism. It has been identified that the charge transport in blue phosphorescent organic light-emitting diodes is electron dominated and the decrease of current in degraded devices is due to the formation of electron traps.[14] In this work, by using transient electroluminescence measurements, we disentangle the charge transport in both pristine and degraded quantum dot light-emitting diodes and directly trace the change of unipolar transport in blue QLEDs before and after aging. By changing the thicknesses of the electron transport layer, the hole transport layer, and the emissive quantum dot layer, respectively, we find that the charge transport in pristine QLEDs is primarily governed by holes. Furthermore, a decrease of hole transport in the emissive quantum dot layer is detected in degraded blue QLEDs, which is attributed to the formation of hole traps.

II. EXPERIMENTAL

In this work, we fabricated QLEDs based on $Cd_xZn_{1-x}Se$/ZnSe/CdZnS/ZnS blue quantum dots (QDs).[16] In these devices, poly((9,9-dioctylfluorenyl-2,7-diyl)-co-{4,4′-[N-(4-sec-butylphenyl) diphenylamine]}) (TFB) was employed as the hole transport layer (HTL), magnesium doped zinc oxide (ZnMgO) nanoparticles were employed as the electron transport layer (ETL), and poly (3,4-ethylenedioxythiophene):poly(styrenesulfonate) (PEDOT:PSS) was employed as the hole injection layer (HIL). The corresponding device architectures used in this study were indium tin oxide (ITO)/HIL (20 nm)/TFB (x nm)/QDs (y nm)/ZnMgO (z nm)/Ag (100 nm), as shown in Fig. 1(a). The normalized electroluminescence (EL) spectrum of the device is shown in Fig. 1(b). The EL spectrum exhibits a narrow peak at 476 nm with full-width at half-maximum of 16 nm. The energy band diagram of the device is schematically shown in Fig. 1(c).[3,8,16–19] The valence band maximum (VBM) of the ZnMgO electron transport layer was measured as −6.66 eV by photoemission yield spectroscopy. The optical bandgap was determined to be −3.53 eV by the absorption spectra. According to the measured valence band maximum and the optical bandgap, the conduction band minimum (CBM) of ZnMgO was calculated to be −3.13 eV. In this study, the thicknesses of the charge transport layers and the emissive layer (EML) were changed. The thicknesses of HTL, ETL, and EML of these devices are illustrated in Fig. 1(d). In devices A, B, and C with 35 nm ETL, the thickness of HTL is 13, 27, and 44 nm, respectively. In devices D, E, and F with 25 nm HTL, the thickness of ETL is 34, 44, and 58 nm, respectively. For the above devices, the thickness of EML remained the same at 35 nm. In devices G, H, and I, the thickness of the emissive layer is 30, 55, and 68 nm, combined with 25 nm HTL and 35 nm ETL. Finally, all the samples were loaded into a high-vacuum chamber for deposition of an Ag cathode (100 nm), patterned by a shadow mask to form an active device area of 0.04 cm^2. All devices were fabricated in a nitrogen atmosphere and were encapsulated with glass to protect the devices from oxygen and water.

In order to study the transport properties of $Cd_xZn_{1-x}Se$/ZnSe/CdZnS/ZnS blue quantum dots, we fabricated hole-only devices and electron-only devices, with the structures of ITO/PEDOT:PSS (40 nm)/QDs (100 nm)/molybdenum trioxide (MoO_3) (10 nm)/Al (100 nm) and Al (30 nm)/QDs (100 nm)/lithium fluoride (LiF) (1 nm)/Al (100 nm), respectively. In the hole-only devices, the emissive quantum dot layer is sandwiched between two high-work-function electrodes (PEDOT:PSS and MoO_3). This structure only allows the injection of holes, and the large injection barrier for electrons prevents electron injection from electrodes into the quantum dot layer. Likewise, electron-only devices only allow electrons to be injected into the quantum dot layer from the

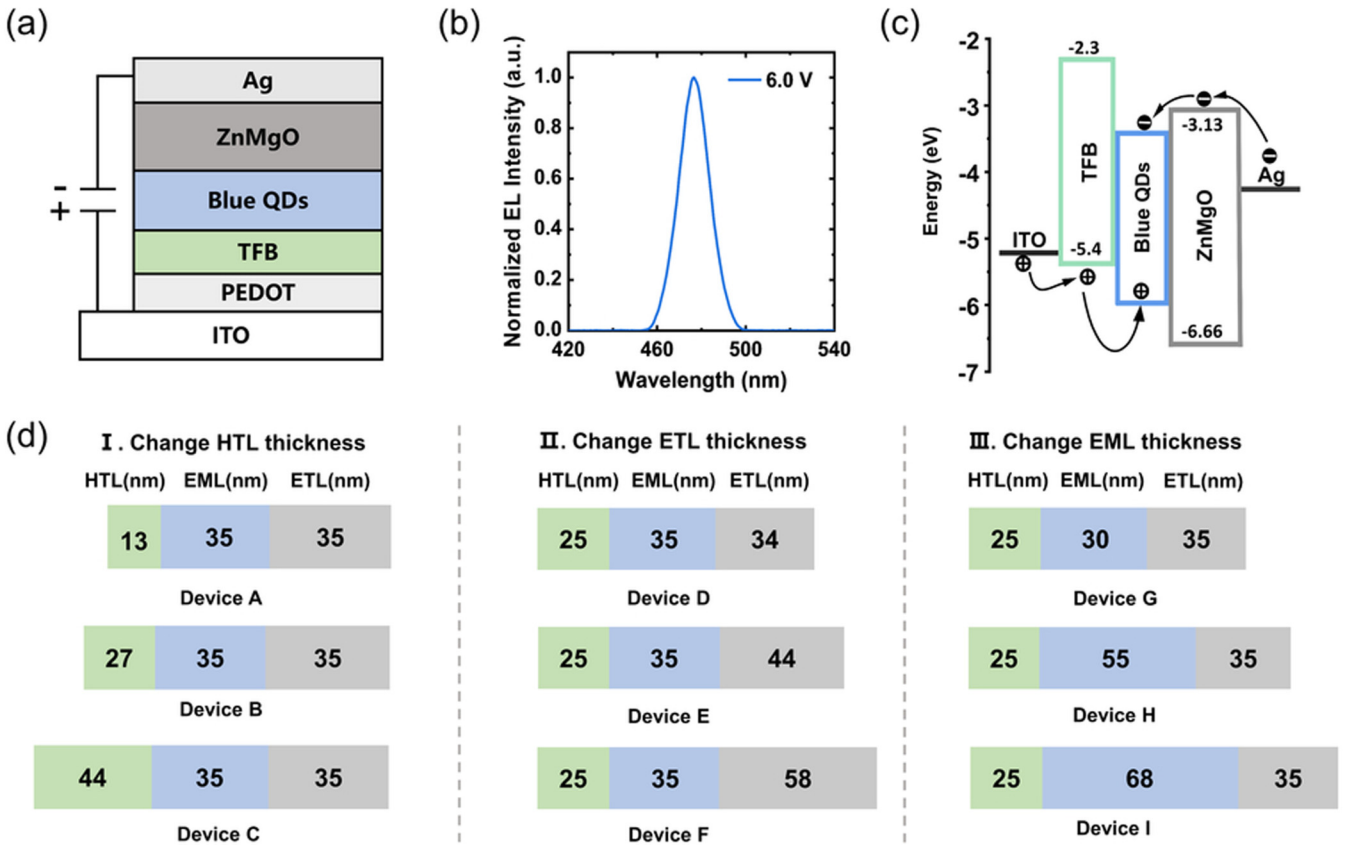

FIG. 1. (a) Schematic device structure of the blue QLED based on $Cd_xZn_{1-x}Se/ZnSe/CdZnS/ZnS$ quantum dots [ITO/HIL/HTL (27 nm)/QDs (35 nm)/ETL (35 nm)/Ag]. (b) Normalized electroluminescence spectrum of the blue QLED measured at the voltage of 6.0 V. (c) Energy level of the diagram of blue QLEDs.[3,8,16–19] (d) Blue QLED structures with various thicknesses of HTL (device I), ETL (device II), and EML (device III).

LiF/Al and the Al contacts, and these two electrodes prevent hole injection into the quantum dot layer. Therefore, no recombination occurs and no photon is generated in both hole-only devices and electron-only devices.

The measurements were performed in an inert-atmosphere (<0.1 ppm O_2 and H_2O) glovebox. The current density–voltage–light output (J–V–L) characteristics were measured with a Keithley 2400 source meter and an electrometer Keithley 6514 monitoring the photocurrent (light output) of a calibrated Si photodiode. The conversion efficiency is defined as the light output divides the device current. In transient electroluminescence (TEL) measurements, a voltage pulse was applied to QLEDs using a pulse generator to emit light. The integrated light output (I_{out}) was measured using a Keithley 6514 electrometer in the current mode. The time resolution of TEL measurements is limited by the resistor–capacitance (RC) time constant of each QLED circuit.[13] At a voltage of 6 V, the time resolution was found to be approximately 0.3 μs for various devices. In the aging tests, the devices were stressed under a constant current density ($J = 50$ mA/cm^2) in the glovebox.

III. TRANSIENT ELECTROLUMINESCENCE MEASUREMENTS

A. Principle

To study the charge transport in multi-layer QLEDs, we applied transient electroluminescence (TEL) measurements on QLEDs to determine the transit time of charge carriers. Different from the time-of-flight (TOF) technique that is typically performed on a thick semiconductor film (~μm), transient electroluminescence measurements can be used in conventional light-emitting diodes with thin active layers (~100 nm).[14,15] In TEL measurements, there is a time lag between the application of a voltage pulse and the onset of the electroluminescence (EL) of devices [Fig. 2(a)]. In our devices, holes and electrons are injected into the semiconductors after applying voltage and then flow toward each other under the electric field and recombine for the light output.[13] Thus, the observed time lag (τ) is equal to the transit time of charge carriers. For a semiconductor layer between two electrodes, the thickness L is the sum of the transport distance of the injected electrons and holes, given by $L_e = E \times \mu_e \times \tau$ and $L_h = E \times \mu_h \times \tau$, respectively,

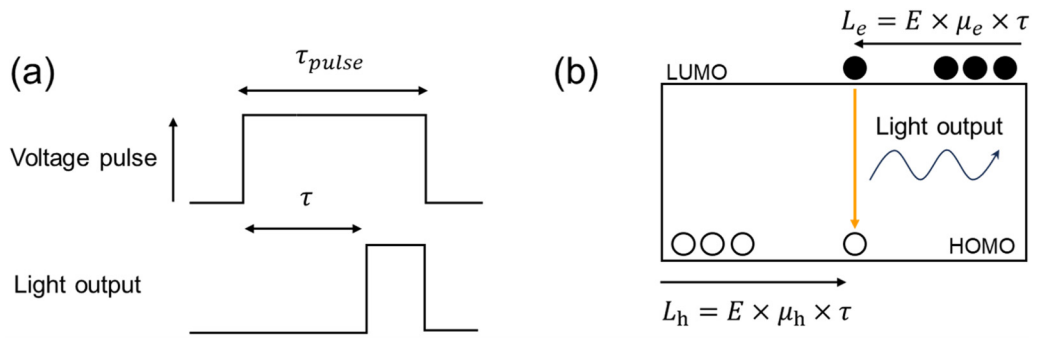

FIG. 2. (a) A schematic representation of QLED exhibiting a time lag τ between the application of a voltage pulse and the first observation of light output. (b) Schematic charge transport and recombination in transient electroluminescence measurement. (The hollow circles represent the holes, and the black circles represent the electrons.)

with E being the electric field, μ_e and μ_h being the mobility of electrons and holes [Fig. 2(b)]. Then, the transit time (τ) is given by $\tau = L/(E \times (\mu_e + \mu_h))$.[14] Furthermore, two limiting cases for the transit time are considered. In case that charge transport is unbalanced and $\mu_h \gg \mu_e$, the recombination is confined to a region close to the cathode, thus the measured transit time τ is determined by the transit time of holes, given by $\tau = L/(E \times \mu_h)$. Conversely, when $\mu_e \gg \mu_h$, the measured transit time τ represents the transit time of electrons. In other words, the measured transit time τ is correlated with the transit time of the fastest charge carrier for unbalanced transport.

Experimentally, a voltage pulse with a width (τ_{pulse}) of range from 2 to 200 μs was applied to the devices at a repetition frequency of 1 kHz using a pulse generator. The integrated light output (I_{out}) was measured using a Keithley 6514 electrometer in the current mode. When the pulse width is comparable to τ, the integrated light output I_{out} is relatively small. With increasing pulse width, I_{out} increases strongly, and when τ_{pulse} is much longer than τ, I_{out} vs τ_{pulse} approaches a linear behavior. The intercept of the linear part with the τ_{pulse}-axis is then a measure for the transit time τ.[13,14]

B. Operation of the pristine device

In current QLEDs [Fig. 1(a)], since the transit time reflects the charge injection and transport processes, it should be divided into the injection time ($\tau_{injetcion}$) and the transport time ($\tau_{transport}$), represented as $\tau = \tau_{injetcion} + \tau_{transport}$. Here, $\tau_{injetcion}$ is the sum of time for charge carriers to inject into the charge transport layers and the emissive layer. As shown in Fig. 1(c), there is a large hole injection barrier due to the mismatch between the deep valance band of blue QD (−6.2 eV)[16] and the highest occupied molecular orbital (HOMO) of TFB (−5.4 eV).[3] As a result, $\tau_{injetcion}$ is dominantly taken for hole injection from the hole transport layer into the emissive layer. As for $\tau_{transport}$, it is composed of the time for charge carriers to flow from the electrode to the recombination zone.

To disentangle the contributions of electron and hole transport in different layers on the transit time, we changed the thicknesses of the electron transport layer, the hole transport layer, and the emissive quantum dot layer of QLEDs, respectively, and the corresponding transit time was recorded by using transient electroluminescence measurements. For example, the result of TEL measurements on a pristine device consisting of 25 nm HTL, 30 nm EML, and 35 nm ETL is presented in Fig. 3. The integrated light output as a function of pulse width is recorded for various applied voltages. The intercept of the linear part at long pulse widths with the τ_{pulse}-axis indicates the transit time. In Fig. 4, the measured transit time is plotted as a function of voltage for QLEDs with varying thicknesses of the electron transport layer (a), the hole transport layer (b), and the emissive layer (c), respectively. The integrated light output as a function of pulse width corresponding to Fig. 4 is shown in Fig. S1 in the supplementary material. Figure 4(a) shows that when the thickness of the electron transport layer increases from 34 to 58 nm, the transit time increases around 1.6 times at a voltage of 5 V. We need to notice that the increase of ETL thickness will not only increase the transport distance of electrons but also reduce the electric field intensity. Assuming that the transport is dominated by the electrons in the electron transport layer, when the thickness of the electron transport layer increases from 34 to 58 nm, the transport distance of charge carriers in the electron transport layer will extend by 1.6 times and the electric field intensity $E = (V - V_{bi})/d$ (with V being the applied voltage, V_{bi} being the built-in voltage, and d being the thickness of devices) will decrease by 1.3 times. According to the equation $\tau = L/(E \times \mu)$, the transit time τ is expected to rise at least two times. However, the measured transit time only increases by 1.6 times at a voltage of 5 V [Fig. 4(a)]. Therefore, the transport cannot be dominated by the electron transport in the electron transport layer. As shown in Fig. 4(b), when the thickness of the hole transport layer triples from 13 to 44 nm, the transit time only increases by 1.2 times at a voltage of 5 V. Different from the slight change in the transit time when varying the thickness of the electron transport layer and the hole transport layer, respectively, a significant increase in the transit time is observed when varying the thickness of the emissive quantum dot layer. As Fig. 4(c) shows, when doubling the thickness of the emissive layer from 30 to 68 nm, a fourfold increase in the transit time τ at a voltage of 5 V is observed. It

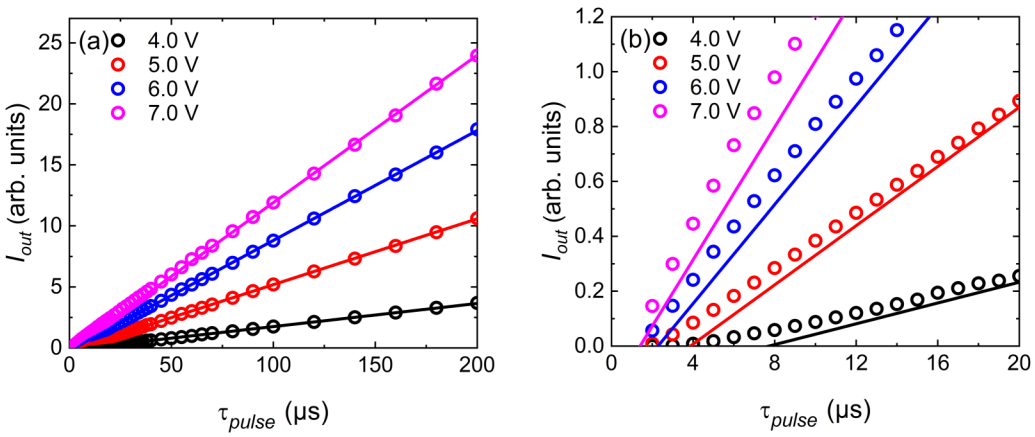

FIG. 3. (a) Integrated light output I_{out} vs pulse width τ_{pulse} of a pristine blue QLED [structure: ITO/HIL/HTL (25 nm)/QDs (30 nm)/ETL (35 nm)/Ag]. The symbols correspond to the measured integrated light output for various applied voltages. The solid lines are linear fits to the data at long pulse widths, and their intercept with the τ_{pulse}-axis corresponds to the measured transit time τ. (b) An enlarged plot of I_{out} vs τ_{pulse} at short pulse widths.

can be interpreted as follows. When the thickness of the emissive layer increases from 30 to 68 nm, the transport distance of charge carriers L in the emissive layer extends 2.3 times, at the same time, the electric field intensity $[E = (V - V_{bi})/d]$ decreases by 1.4 times. Moreover, the mobility of charge carriers in quantum dots is found to be dependent on the electric field (Fig. 5). The decrease in the electric field by 1.4 times leads to a decrease in mobility by 1.3 times. The electric field dependence of mobility will be discussed in more detail in the next three paragraphs. According to the equation $\tau = L/(E \times \mu)$, the transit time then increases by four times, instead of increasing by 2.3 times. This fourfold increase is consistent with the increased transit time as obtained from TEL measurements. Thereby, the measured transit time recorded from TEL measurements is determined by the charge transport in the emissive quantum dot layer, instead of the electron and hole transport layers.

We note that when varying the thickness of the hole transport layer, the change in the transit time τ is relatively smaller than that when changing the thickness of the electron transport layer. It can be due to the fact that the accumulated electrons at the interface between the hole transport layer and the quantum dot layer (HTL/QD) enhance hole injection, as reported in the past.[20–24] Since the valence band maximum of blue quantum dots is relatively deep, it does not well-align with the highest occupied molecular orbital (HOMO) of the hole transport layer TFB.[3,16] This misalignment leads to a hole injection barrier, hindering efficient hole injection and leading to hole accumulation at the interface between the hole transport layer and the quantum dot layer. In order to balance the excess space charge, the injected electrons reach the interface between the hole transport layer and the quantum dot layer and get trapped at the interface.[20–24] Subsequently, the accumulated electrons could enhance hole injection through the following two processes. (a) The trapped electrons increase the electric field across the HTL/QD interface, thus facilitating the injection of holes.[20,24] (b) The trapped electrons give rise to a strong dipole across a thin injection barrier present at the HTL/QD interface. When the dipole is sufficiently large, holes can directly tunnel from the hole transport layer to the transport states of the light-emitting materials.[21–23] In this way, the accumulated electrons at the HTL/QD interface enhance hole injection and improve the charge balance. Since electrons need to be transported through the electron transport layer to reach the HTL/QD interface, when the thickness of the electron transport layer reduces, the transport distance of electrons decreases, and, thus, more electrons arrive and accumulate at the HTL/QD interface per unit time, which enhance the injection of holes from the hole transport layer to the quantum dot layer and accelerate the hole injection process. Thereby, $\tau_{injetcion}$ decreases, which leads to a decrease in the transit time, as $\tau = \tau_{injetcion} + \tau_{transport}$. While for devices with various thicknesses of the hole transport layer, the transit distance of electrons to reach the HTL/QD interface is unchanged. Therefore, the injection time $\tau_{injetcion}$ shows less deviation, resulting in a relatively less change in the transit time τ.

Since we can use TEL measurements to directly observe the transit time of charge transport in the emissive quantum dot layer, the next step is to understand which type of charge carriers plays a dominant role in charge transport in QLEDs. From TEL measurements, the mobility of charge carriers in the emissive quantum dot layer in a pristine QLED can be calculated as[13,14]

$$\mu = \frac{L_{EML}}{E \times \tau}, \tag{1}$$

where τ is the measured transit time, L_{EML} is the thickness of the emissive layer, and E is the average electric field given by $E = (V - V_{bi})/d$, with V being the applied voltage, V_{bi} being the built-in voltage, and d being the thickness of devices.[13] Here, the built-in voltage V_{bi} can be calculated from the offset between the Fermi energy of the transport layers,[25–28] which was calculated as

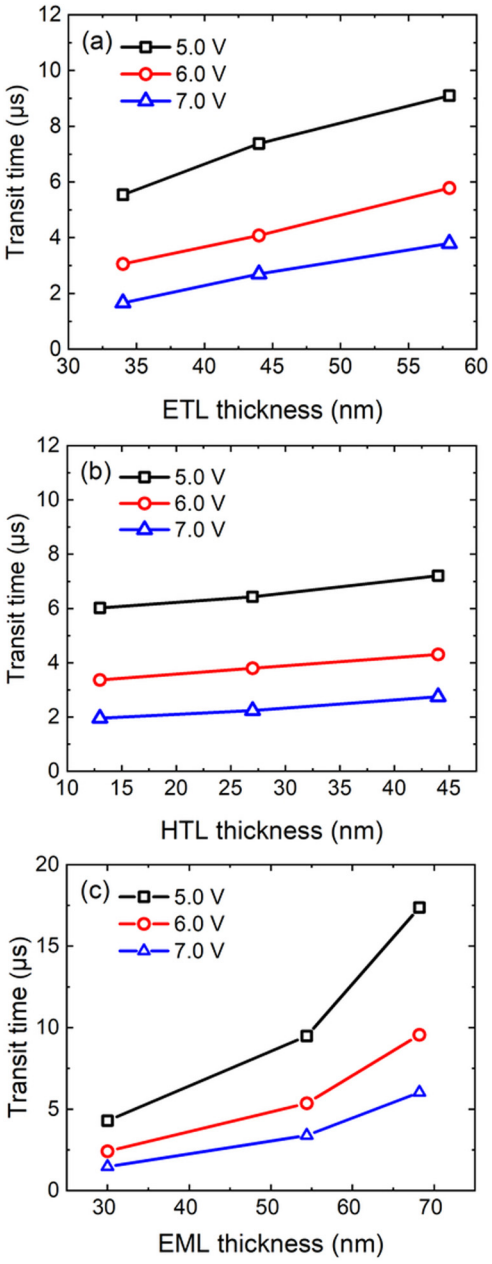

FIG. 4. (a) The transit time of pristine QLEDs with different thicknesses of electron transport layers. (b) The transit time of pristine QLEDs with different thicknesses of hole transport layers. (c) The transit time of pristine QLEDs with different thicknesses of emissive layers.

2.0 V.[29,30] Since the transit time τ is dominated by the charge transport time in the emissive layer, as mentioned above, the injection time can be neglected to simplify the calculation.[13,31] Using Eq. (1), for QLEDs with different functional layer thicknesses, the mobility

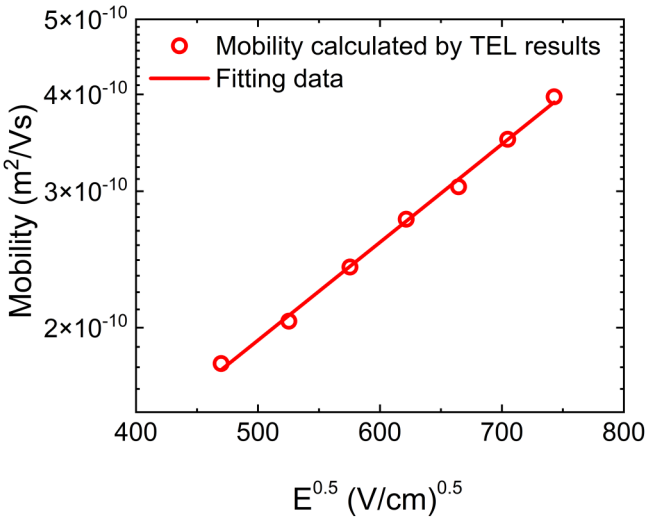

FIG. 5. Mobility calculated from the observed transit time as a function of the square of the electric field in a QLED [ITO/HIL/TFB (25 nm)/QDs (30 nm)/ZnMgO (35 nm)/Ag].

of the fastest charge carrier in the emissive layer is estimated as $1.51–2.35 \times 10^{-10}$ m^2/Vs at a voltage of 5 V, with the order of magnitude independent of the thickness of each functional layer individually, as shown in Table I. These values are two or three magnitudes lower than the mobility of TFB ($\sim 10^{-7}$ m^2/V s)[32] and ZnMgO ($\sim 10^{-8}$ m^2/V s),[33,34] which further indicates that the transit time as obtained corresponds to the charge transport in the emissive quantum dot layer, instead of the electron and hole transport layers.

We also find that the mobility in quantum dots is electric field dependent. For example, the mobility for a QLED [ITO/HIL/TFB (25 nm)/QDs (30 nm)/ZnMgO (35 nm)/Ag] was calculated by Eq. (1) and its electric field dependence is plotted in Fig. 5. Within the range of the electric field from 2.21×10^5 to 5.52×10^5 V/cm, the mobility ranges from 1.80×10^{-10} to 3.97×10^{-10} m^2/Vs. The logarithm of mobility is proportional to the square root of the electric field. This electric field dependence follows the Poole–Frenkel effect, which is a common phenomenon in the energy-disordered system, i.e., organic semiconductors,[35,36] given by[35]

$$\mu = \mu_0 \exp\left(\gamma\sqrt{E}\right), \tag{2}$$

where μ_0 denotes the mobility at zero field and γ is the coefficient. By fitting the experimental data with Eq. (2), we determined that the value of the zero-field mobility μ_0 is 4.49×10^{-11} m^2/Vs, while the value of coefficient γ is 2.91×10^{-3} cm$^{1/2}$/V$^{1/2}$.

To further understand the obtained mobility corresponds to which type of charge carriers in the quantum dot emissive layer, we fabricated single-carrier devices based on $Cd_xZn_{1-x}Se$/ZnSe/CdZnS/ZnS blue quantum dots. For this, we fabricated hole-only devices and electron-only devices, with the structures of ITO/PEDOT:PSS/QDs (100 nm)/MoO_3/Al and Al/QDs (100 nm)/LiF/Al, respectively. As shown in Fig. 6, the hole current shows three

TABLE I. The calculated mobility of devices with different thicknesses of ETL, HTL, and EML.

	Mobility (m^2/Vs)		
Devices with different thicknesses of ETL	At 5.0 V	At 6.0 V	At 7.0 V
Device D: 25 nm HTL + 35 nm QD + 34 nm ETL	1.98×10^{-10}	2.69×10^{-10}	3.96×10^{-10}
Device E: 25 nm HTL + 35 nm QD + 44 nm ETL	1.65×10^{-10}	2.22×10^{-10}	2.70×10^{-10}
Device F: 25 nm HTL + 35 nm QD + 58 nm ETL	1.51×10^{-10}	1.79×10^{-10}	2.18×10^{-10}
	Mobility (m^2/Vs)		
Devices with different thicknesses of HTL	At 5.0 V	At 6.0 V	At 7.0 V
Device A: 13 nm HTL + 35 nm QD + 35 nm ETL	1.61×10^{-10}	2.18×10^{-10}	2.71×10^{-10}
Device B: 27 nm HTL + 35 nm QD + 35 nm ETL	1.76×10^{-10}	2.23×10^{-10}	3.03×10^{-10}
Device C: 44 nm HTL + 35 nm QD + 35 nm ETL	1.84×10^{-10}	2.31×10^{-10}	2.94×10^{-10}
	Mobility (m^2/Vs)		
Devices with different thicknesses of EML	At 5.0 V	At 6.0 V	At 7.0 V
Device G: 25 nm HTL + 30 nm QD + 35 nm ETL	2.15×10^{-10}	2.86×10^{-10}	3.76×10^{-10}
Device H: 25 nm HTL + 55 nm QD + 35 nm ETL	2.35×10^{-10}	3.06×10^{-10}	3.83×10^{-10}
Device I: 25 nm HTL + 68 nm QD + 35 nm ETL	1.94×10^{-10}	2.54×10^{-10}	3.15×10^{-10}

orders of magnitude larger than the electron current, indicating a more efficient transport of holes compared to that of electrons. *J*–*V* characteristics of the hole-only device can be described by space-charge limited current (SCLC), as expressed in[35]

$$J = \frac{9}{8}\varepsilon\varepsilon_0\mu\frac{V^2}{L^3}, \tag{3}$$

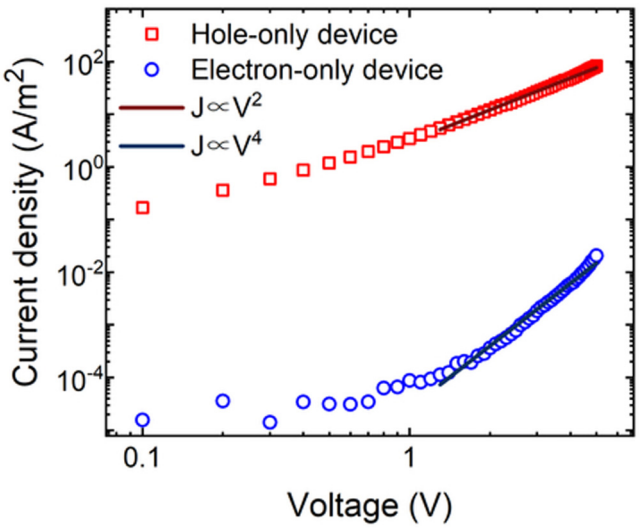

FIG. 6. Current density–voltage characteristics for the hole-only device and the electron-only device with 100 nm thin films of $Cd_xZn_{1-x}Se/ZnSe/CdZnS/ZnS$ quantum dots.

where μ is the field-dependent mobility described by Eq. (2) and ε and ε_0 are the relative dielectric constant and free-space permittivity, respectively.[35] By setting the relative dielectric constant of the $Cd_xZn_{1-x}Se/ZnSe/CdZnS/ZnS$ quantum dots $\varepsilon = 9.4$,[37] a zero-field hole mobility of 2.80×10^{-11} m^2/Vs is obtained, which is similar to the mobility as obtained by TEL measurements of 4.49×10^{-11} m^2/Vs. It indicates that the mobility as obtained by TEL measurements corresponds to the mobility of holes and the observed charge transport in QLEDs is hole dominated.

This result contradicts some previous views that charge transport in QLEDs is dominated by electrons.[11,38] It was believed that the electron mobility of inorganic electron transport materials (i.e., ZnO) is higher than the hole mobility of organic hole transport materials (i.e., TFB).[38] Moreover, the injection barrier for holes is larger than that for electrons.[11,38] However, the charge transport within quantum dot thin films has not been discussed yet in those works.

It was also argued that the hole current in quantum dots is higher than the electron current, as investigated based on single-carrier devices.[2,39] As Fig. 6 shows, the electron current of quantum dots is at least three orders of magnitude lower compared to the hole current. Moreover, the hole current depends quadratically on voltage, which signifies the trap-free space-charge limited hole transport in quantum dots.[40] While the electron current shows a stronger voltage dependence, typically $J \sim V^4$, which is a distinctive feature of trap-limited currents.[40] Such a significant reduction of electron current in quantum dots due to the existence of electron traps further supports the hole dominant transport in quantum dot light-emitting diodes.

C. TEL measurements of the degraded devices

To further investigate the degradation mechanism and trace the charge transport of QLEDs before and after aging, blue QLEDs

based on $Cd_xZn_{1-x}Se/ZnSe/CdZnS/ZnS$ quantum dots [Fig. 1(a)] were stressed at a constant current density of 50 mA/cm^2, and the J–V characteristics and conversion efficiencies of devices under different aging periods (from 30 min to 100 h) were recorded, as depicted in Fig. 7. After long-term stress, the current density decreases gradually, especially in the low-voltage regime, and recovers somehow at higher voltages [Fig. 7(a)]. The conversion efficiency of devices increases during the initial 1.5 h, which is attributed to the enhanced hole injection and more balanced charge transport.[22] When stressed for longer periods, a reduction of efficiency with aging time is observed [Fig. 7(b)]. The change in the charge transport and the recombination process of blue QLEDs upon aging was investigated using TEL measurements. Figure 8 shows the transit time of QLEDs as a function of aging periods under the voltage of 5.0–6.5 V. The transit time decreases by 30%–44% during the first 30 min of aging [Fig. 8(a)]; such a decrease in the transit time is due to the enhancement of hole injection and balanced charge transport.[22] After that, the transit time increases with aging time for longer aging periods, as Fig. 8(b) represents. After aging for 100 h, the transit time shows a fourfold increase at a voltage of 5 V, corresponding to the decrease in device current by

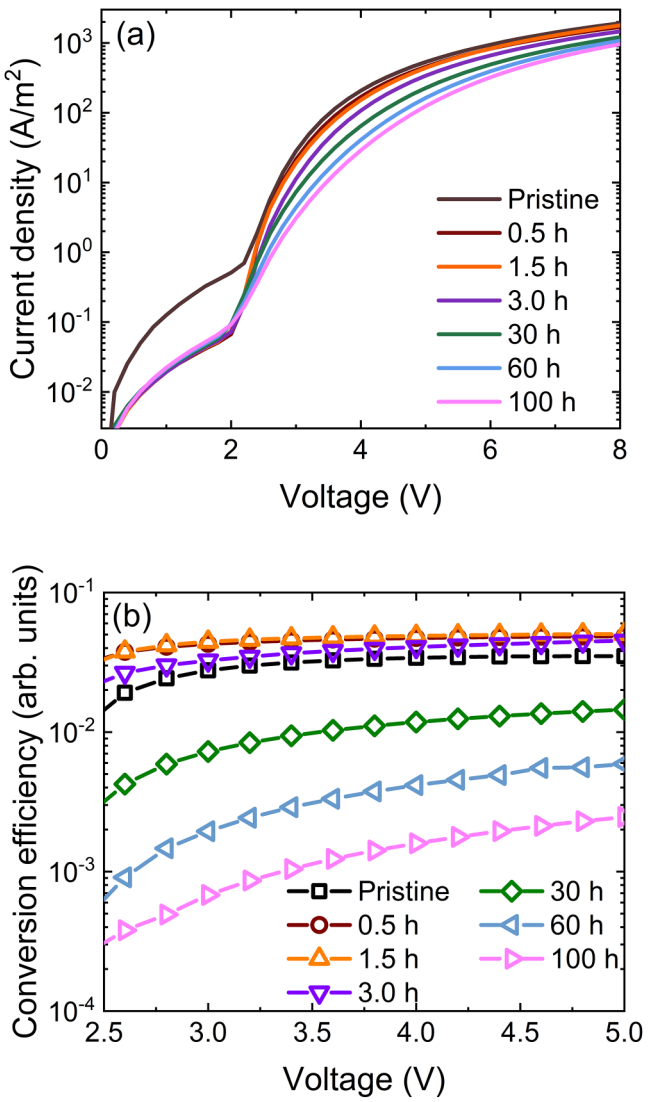

FIG. 7. (a) Current density vs voltage and (b) conversion efficiency vs voltage for blue QLED consisting of 27 nm HTL, 35 nm QDs, and 35 nm ETL, stressed at 50 mA/cm^2 for different periods of time.

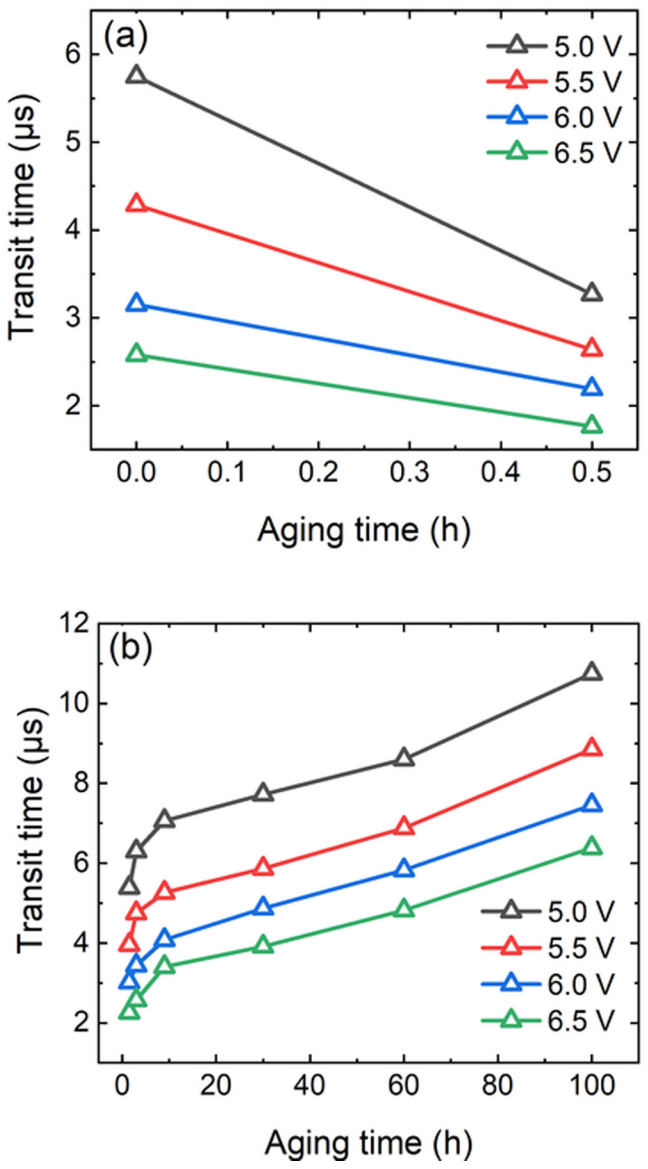

FIG. 8. Evolution of the transit time during electrical aging of QLED consisting of 27 nm HTL, 35 nm QDs, and 35 nm ETL under a constant current density of 50 mA/cm^2 (a) for short aging periods and (b) for longer aging periods.

72%, indicating that the increase in the measured transit time has a strong correlation with the decrease in current density upon aging of QLEDs.

Since the measured transit time represents the hole transport in the emissive quantum dot layer, the observed increase in the transit time indicates that the hole transport in the quantum dot layer decreases upon electrical aging.

There are two possibilities to explain the hole transport decrease. One possible reason can be the reduction in hole mobility. In this case, the current of the device decreases in both low-voltage and high-voltage regimes. However, as Fig. 7(a) shows, the current of the degraded device decreases strongly at low voltages and recovers at higher voltages. It is a fingerprint for trap-limited transport.[15] Moreover, Fig. 7(b) shows that the conversion efficiency decreases by around 90% for 100 h aged devices compared to pristine ones. As the conversion efficiency is defined as the light output divides the device current, both these are proportional to the charge mobility, meaning the efficiency itself is independent of mobility.[41] Therefore, the decrease in charge mobility can be ruled out as the reason for the significant decrease in efficiency. The other possibility is that the generated hole traps can even act as dark recombination sites or exciton quenchers. It is supported by the J–V characteristics of degraded QLEDs. In Fig. 7(a), strong current reduction especially at the low-voltage regime and recovery in the higher voltage regime is a fingerprint for trap-limited currents,[15] indicating that trap-assisted recombination occurs and plays a significant role in degraded devices. Additionally, due to the significant reduction of device efficiency during long-term aging, the hole traps not only play a role in hindering the charge transport and decreasing the device current, but also lead to additional trap-assisted recombination and act as exciton quenchers, which together decrease device efficiency. Considering that blue quantum dots have a high surface-to-volume ratio, these traps could probably originate from the surface defects on quantum dots.[42,43]

IV. CONCLUSION

In summary, the charge transport in blue quantum dot light-emitting diodes based on $Cd_xZn_{1-x}Se/ZnSe/CdZnS/ZnS$ quantum dots was investigated using transient electroluminescence measurements. By varying the thicknesses of the electron transport layer, the hole transport layer, and the emissive layer, respectively, it has been shown that the charge transport in the quantum dot light-emitting diodes is dominated by holes. The mobility of hole transport in the quantum dot emissive layer can be extracted, which exhibits an electric field dependence with the zero-field mobility $\mu_0 = 4.49 \times 10^{-11}\ m^2/Vs$ and the field-dependent coefficient $\gamma = 2.91 \times 10^{-3}\ cm^{1/2}/V^{1/2}$. Furthermore, for blue QLEDs after long-term electrical aging, the reduction of device current is consistent with the decrease of hole transport in the emissive quantum dot layer, which is attributed to the formation of hole traps. The hole traps not only play a role in decreasing the device current, but also lead to additional trap-assisted recombination that decreases the efficiency of degraded blue quantum dot light-emitting diodes. This result will enable us to evaluate how the formation of traps depends on the aging conditions and with which process it correlates, in a further study. Such information is essential to unravel the degradation mechanism of QLEDs, paving the way toward stable blue QLEDs.

SUPPLEMENTARY MATERIAL

See the supplementary material for the integrated light output as a function of pulse widths of blue quantum dot light-emitting diodes with various thicknesses of the electron transport layer, the hole transport layer, and the emissive layer, respectively.

ACKNOWLEDGMENTS

This work was funded by TCL Corporate Research, the National Natural Science Foundation of China (No. 52103207), the Natural Science Foundation of Guangdong Province (No. 2022A1515011969), and the Fundamental Research Funds for the Central Universities (No. 2023ZYGXZR025).

AUTHOR DECLARATIONS

Conflict of Interest

The authors have no conflicts to disclose.

Author Contributions

W.L., J.H., and S.L. contributed equally to this work.

Wenxin Lin: Data curation (equal); Formal analysis (equal); Investigation (equal); Writing – original draft (equal). **Jiangxia Huang:** Data curation (equal); Formal analysis (equal); Investigation (equal); Writing – original draft (equal). **Shuxin Li:** Formal analysis (equal); Investigation (equal); Writing – review & editing (equal). **Paul W. M. Blom:** Supervision (equal); Writing – review & editing (equal). **Haonan Feng:** Data curation (equal); Formal analysis (equal); Investigation (equal); Writing – review & editing (supporting). **Jiahao Li:** Data curation (equal); Formal analysis (equal); Investigation (equal). **Xiongfeng Lin:** Investigation (equal); Resources (equal). **Yulin Guo:** Investigation (equal); Resources (equal). **Wenlin Liang:** Investigation (equal); Resources (equal). **Longjia Wu:** Investigation (equal); Resources (equal). **Quan Niu:** Conceptualization (equal); Formal analysis (equal); Funding acquisition (equal); Methodology (equal); Project administration (equal); Supervision (equal); Writing – review & editing (equal). **Yuguang Ma:** Supervision (equal); Writing – review & editing (equal).

DATA AVAILABILITY

The data that support the findings of this study are available from the corresponding author upon reasonable request.

REFERENCES

[1]J. H. Chang, P. Park, H. Jung, B. G. Jeong, D. Hahm, G. Nagamine, J. Ko, J. Cho, L. A. Padilha, D. C. Lee, C. Lee, K. Char, and W. K. Bae, "Unraveling the origin of operational instability of quantum dot based light-emitting diodes," ACS Nano **12**, 10231–10239 (2018).

[2]C. Xiang, L. Wu, Z. Lu, M. Li, Y. Wen, Y. Yang, W. Liu, T. Zhang, W. Cao, S. W. Tsang, B. Shan, X. Yan, and L. Qian, "High efficiency and stability of ink-jet printed quantum dot light emitting diodes," Nat. Commun. **11**, 1646 (2020).

[3]Y. Deng, F. Peng, Y. Lu, X. Zhu, W. Jin, J. Qiu, J. Dong, Y. Hao, D. Di, Y. Gao, T. Sun, M. Zhang, F. Liu, L. Wang, L. Ying, F. Huang, and Y. Jin, "Solution-processed green and blue quantum-dot light-emitting diodes with eliminated charge leakage," Nat. Photonics **16**, 505–511 (2022).
[4]C. Pu, X. Dai, Y. Shu, M. Zhu, Y. Deng, Y. Jin, and X. Peng, "Electrochemically-stable ligands bridge the photoluminescence-electroluminescence gap of quantum dots," Nat. Commun. **11**, 937 (2020).
[5]H. Shen, Q. Gao, Y. Zhang, Y. Lin, Q. Lin, Z. Li, L. Chen, Z. Zeng, X. Li, Y. Jia, S. Wang, Z. Du, L. S. Li, and Z. Zhang, "Visible quantum dot light-emitting diodes with simultaneous high brightness and efficiency," Nat. Photonics **13**, 192–197 (2019).
[6]Y. Yang, Y. Zheng, W. Cao, A. Titov, J. Hyvonen, J. R. Manders, J. Xue, P. H. Holloway, and L. Qian, "High-efficiency light-emitting devices based on quantum dots with tailored nanostructures," Nat. Photonics **9**, 259–266 (2015).
[7]D. Liu, S. Cao, S. Wang, H. Wang, W. Dai, B. Zou, J. Zhao, and Y. Wang, "Highly stable red quantum dot light-emitting diodes with long T_{95} operation lifetimes," J. Phys. Chem. Lett. **11**, 3111–3115 (2020).
[8]S. Chen, W. Cao, T. Liu, S. Tsang, Y. Yang, X. Yan, and L. Qian, "On the degradation mechanisms of quantum-dot light-emitting diodes," Nat. Commun. **10**, 765 (2019).
[9]W. Cao, C. Xiang, Y. Yang, Q. Chen, L. Chen, X. Yan, and L. Qian, "Highly stable QLEDs with improved hole injection via quantum dot structure tailoring," Nat. Commun. **9**, 2608 (2018).
[10]A. Liu, C. Cheng, and J. Tian, "Exploring performance degradation of quantum-dot light-emitting diodes," J. Mater. Chem. C **10**, 8642–8649 (2022).
[11]H. Moon, C. Lee, W. Lee, J. Kim, and H. Chae, "Stability of quantum dots, quantum dot films, and quantum dot light-emitting diodes for display applications," Adv. Mater. **31**, 1804294 (2019).
[12]T. Davidson-Hall and H. Aziz, "Perspective: Toward highly stable electroluminescent quantum dot light-emitting devices in the visible range," Appl. Phys. Lett. **116**, 010502 (2020).
[13]P. W. M. Blom and M. C. J. M. Vissenberg, "Dispersive hole transport in poly (p-phenylene vinylene)," Phys. Rev. Lett. **80**, 3819–3822 (1998).
[14]Q. Niu, P. W. M. Blom, F. May, P. Heimel, M. Zhang, C. Eickhoff, U. Heinemeyer, C. Lennartz, and N. I. Crăciun, "Transient electroluminescence on pristine and degraded phosphorescent blue OLEDs," J. Appl. Phys. **122**, 185502 (2017).
[15]Q. Niu, G. A. H. Wetzelaer, P. W. M. Blom, and N. I. Crăciun, "Modeling of electrical characteristics of degraded polymer light-emitting diodes," Adv. Electron. Mater. **2**, 1600103 (2016).
[16]X. Chen, X. Lin, L. Zhou, X. Sun, R. Li, M. Chen, Y. Yang, W. Hou, L. Wu, W. Cao, X. Zhang, X. Yan, and S. Chen, "Blue light-emitting diodes based on colloidal quantum dots with reduced surface-bulk coupling," Nat. Commun. **14**, 284 (2023).
[17]L. Xie, J. Yang, W. Zhao, Y. Q. Q. Yi, Y. Liu, W. Su, Q. Li, W. Lei, and Z. Cui, "High-performance inkjet-printed blue QLED enabled by crosslinked and intertwined hole transport layer," Adv. Opt. Mater. **10**, 2200935 (2022).
[18]P. Tang, L. Xie, X. Xiong, C. Wei, W. Zhao, M. Chen, J. Zhuang, W. Su, and Z. Cui, "Realizing 22.3% EQE and 7-fold lifetime enhancement in QLEDs via blending polymer TFB and cross-linkable small molecules for a solvent-resistant hole transport layer," ACS Appl. Mater. Interfaces **12**, 13087–13095 (2020).
[19]A. Prudnikau, H. Roshan, F. Paulus, B. Martín García, R. Hübner, H. Bahmani Jalali, M. De Franco, M. Prato, F. Di Stasio, and V. Lesnyak, "Efficient near-infrared light-emitting diodes based on CdHgSe nanoplatelets," Adv. Funct. Mater. (published online, 2023).
[20]T. van Woudenbergh, P. W. M. Blom, and J. N. Huiberts, "Electro-optical properties of a polymer light-emitting diode with an injection-limited hole contact," Appl. Phys. Lett. **82**, 985–987 (2003).
[21]T. van Woudenbergh, J. Wildeman, P. W. M. Blom, J. J. A. M. Bastiaansen, and B. M. W. Langeveld-Vos, "Electron-enhanced hole injection in blue polyfluorene-based polymer light-emitting diodes," Adv. Funct. Mater. **14**, 677–683 (2004).
[22]A. J. A. B. Seeley, R. H. Friend, and J. Kim, "Trap-assisted hole injection and quantum efficiency enhancement in poly(9,9′ dioctylfluorene-alt-benzothiadiazole) polymer light-emitting diodes," J. Appl. Phys. **96**, 7643–7649 (2004).
[23]D. Poplavskyy, J. Nelson, and D. D. C. Bradley, "Ohmic hole injection in poly (9,9-dioctylfluorene) polymer light-emitting diodes," Appl. Phys. Lett. **83**, 707–709 (2003).
[24]K. Murata, S. Cinà, and N. C. Greenham, "Barriers to electron extraction in polymer light-emitting diodes," Appl. Phys. Lett. **79**, 1193–1195 (2001).
[25]S. Olthof, R. Meerheim, M. Schober, and K. Leo, "Energy level alignment at the interfaces in a multilayer organic light-emitting diode structure," Phys. Rev. B **79**, 245308 (2009).
[26]K. Harada, A. G. Werner, M. Pfeiffer, C. J. Bloom, C. M. Elliott, and K. Leo, "Organic homojunction diodes with a high built-in potential: Interpretation of the current-voltage characteristics by a generalized einstein relation," Phys. Rev. Lett. **94**, 036601.1–036601.4 (2005).
[27]W. Tress, K. Leo, and M. Riede, "Influence of hole-transport layers and donor materials on open-circuit voltage and shape of I–V curves of organic solar cells," Adv. Funct. Mater. **21**, 2140–2149 (2011).
[28]E. Siebert-Henze, V. G. Lyssenko, R. Brückner, M. Riede, K. Leo, P. Ho, M. Niggemann, G. Rumbles, L. Schmidt-Mende, and C. Silva, "Electroabsorption studies of organic p-i-n solar cells: Evaluating the built-in voltage," MRS Proc. **1639**, 701 (2014).
[29]J. S. Shin, T. Y. Kim, S. B. Heo, J. Hong, Y. Park, and S. J. Kang, "Improving the performance of quantum-dot light-emitting diodes via an organic–inorganic hybrid hole injection layer," RSC Adv. **11**, 4168–4172 (2021).
[30]J. H. Kim, C. Y. Han, K. S. Lee, K. S. An, W. Song, J. Kim, M. S. Oh, Y. R. Do, and H. Yang, "Performance improvement of quantum dot-light-emitting diodes enabled by an alloyed ZnMgO nanoparticle electron transport layer," Chem. Mater. **27**, 197–204 (2015).
[31]H. T. Nicolai, G. A. H. Wetzelaer, M. Kuik, A. J. Kronemeijer, B. de Boer, and P. W. M. Blom, "Space-charge-limited hole current in poly(9,9-dioctylfluorene) diodes," Appl. Phys. Lett. **96**, 172107 (2010).
[32]M. Redecker, D. D. C. Bradley, M. Inbasekaran, W. W. Wu, and E. P. Woo, "High mobility hole transport fluorene-triarylamine copolymers," Adv. Mater. **11**, 241–246 (1999).
[33]L. Qian, Y. Zheng, J. Xue, and P. H. Holloway, "Stable and efficient quantum-dot light-emitting diodes based on solution-processed multilayer structures," Nat. Photonics **5**, 543–548 (2011).
[34]H. Moon, W. Lee, J. Kim, D. Lee, S. Cha, S. Shin, and H. Chae, "Composition-tailored ZnMgO nanoparticles for electron transport layers of highly efficient and bright InP-based quantum dot light emitting diodes," Chem. Commun. **55**, 13299–13302 (2019).
[35]P. W. M. Blom, M. J. M. de Jong, and M. G. van Munster, "Electric-field and temperature dependence of the hole mobility in poly(p-phenylene vinylene)," Phys. Rev. B **55**, R656–R659 (1997).
[36]L. S. Cui, S. B. Ruan, F. Bencheikh, R. Nagata, L. Zhang, K. Inada, H. Nakanotani, L. S. Liao, and C. Adachi, "Long-lived efficient delayed fluorescence organic light-emitting diodes using n-type hosts," Nat. Commun. **8**, 2250 (2017).
[37]D. L. Rode, "Electron mobility in II-VI semiconductors," Phys. Rev. B **2**, 4036–4044 (1970).
[38]X. Dai, Z. Zhang, Y. Jin, Y. Niu, H. Cao, X. Liang, L. Chen, J. Wang, and X. Peng, "Solution-processed, high-performance light-emitting diodes based on quantum dots," Nature **515**, 96–99 (2014).
[39]Y. H. Won, O. Cho, T. Kim, D. Y. Chung, T. Kim, H. Chung, H. Jang, J. Lee, D. Kim, and E. Jang, "Highly efficient and stable InP/ZnSe/ZnS quantum dot light-emitting diodes," Nature **575**, 634–638 (2019).
[40]D. Abbaszadeh, A. Kunz, N. B. Kotadiya, A. Mondal, D. Andrienko, J. J. Michels, G. A. H. Wetzelaer, and P. W. M. Blom, "Electron trapping in conjugated polymers," Chem. Mater. **31**, 6380–6386 (2019).
[41]B. Van der Zee, Y. Li, G. J. A. H. Wetzelaer, and P. W. M. Blom, "Efficiency of polymer light-emitting diodes: A perspective," Adv. Mater. **34**, 2108887 (2022).
[42]B. Zhou, M. Liu, Y. Wen, Y. Li, and R. Chen, "Atomic layer deposition for quantum dots based devices," Opto Electron. Adv. **3**, 19004301–19004314 (2020).
[43]H. G. Stunnenberg, M. Vermeulen, and Y. Atlasi, "The coordination chemistry of nanocrystal surfaces," Science **347**, 614–615 (2015).